https://doi.org/10.15255/KUI.2020.076
KUI-44/2021
Original scientific paper
Received December 1, 2020
Accepted February 25, 2021

A Contribution to the Modelling of Fouling Resistance in Heat Exchanger-Condenser by Direct and Inverse Artificial Neural Network

A. Benyekhlef,[a,*] *B. Mohammedi*,[b] *S. Hanini*,[a] *M. Boumahdi*,[a] *A. Rezrazi*,[a] and *M. Laidi*[a*]

[a] Laboratory of Biomaterials and Transport Phenomena (LBMPT), University of Médéa, 26 000, Algeria

[b] Nuclear Research Center of Birine, Djelfa,17 000, Algeria

Abstract

The aim of this study was to predict the *fouling resistance* (*FR*) using the *artificial neural networks* (ANN) approach. An experimental database collected from the literature regarding the fouling of condenser tubes cooling seawater of a nuclear power plant was used to build the ANN model. All models contained 7 inputs: dimensionless condenser cooling seawater temperature, dimensionless inside overall heat transfer coefficient, dimensionless outside overall heat transfer coefficient, dimensionless condenser temperature, dimensionless condenser pressure, dimensionless output power, and dimensionless overall thermal efficiency. Dimensionless fouling resistance was the output. The accuracy of the model was confirmed by comparing the predicted and experimental data. The results showed that ANN with a configuration of 7 input neurons, 7 hidden neurons, and 1 output neuron presented an excellent agreement, with the root mean squared error RMSE $= 3.6588 \cdot 10^{-7}$, average absolute percentage error MAPE $= 0.1295$ %, and high determination coefficient of $R^2 = 0.99996$. After conducting the sensitivity analysis (all input variables had strong effect on the estimation of the fouling resistance), in order to control the fouling, an *inverse artificial neural network* (ANNi) model was established, and showed good agreement in the case of different values of dimensionless condenser cooling seawater temperature.

Keywords

Heat exchanger-condenser, fouling, modelling, artificial neural network, graphical user interface, inverse artificial neural network

1 Introduction

In the process industry, many heat exchangers-condensers are used for refrigeration. The accumulation of unwanted deposits on the heat exchanger surfaces is generally called fouling. Fouling is a major problem in condensers and heat exchangers. The existence of these deposits resists the transfer of heat, and thus decreases its effectiveness. All industrial circuits cooled with water are affected by the phenomenon of biological fouling consisting of the growth of biofilms and the settlement of several types of living organisms.

There are few articles published in the literature to identify the fouling phenomenon and its impacts, and few have tried to quantify them.

Eguía et al.[1] attempted to show the growth of biological fouling inside the cooling tubes of an exchanger-condenser, keeping the temperature of the wall constant and using seawater. *Zubair et al*.[2] presented a discussion based on the economic aspects of the fouling of heat exchangers, followed by the thermoeconomic analysis based on the risks of the heat exchanger. *Casanueva et al*.[3] studied the development, growth, and control of marine biological fouling in condenser heat exchangers in order to assess the impact of new regulations on the particular plant and site. *Qureshi et al*.[4] studied the effect of fouling on the thermo-hydraulic characteristics of the heat exchanger. *Durmayaz et al*.[5] proposed a theoretical model to determine the functional relationship between the temperature of the cooling water and the pressure of the condenser on the efficiency of a pressurized water reactor nuclear power plant. *Nebot et al*.[6] presented a model for predicting the maximum value of the thermal resistance of the fouling layer on the steam condensers of power plants cooled with seawater under different conditions: effect of the water velocity and the material of the tube. *Walker et al*.[7] presented a study with three specific objectives: (1) to quantify the economic impact of the fouling condensers for a 550 MW power plant with moderate temperature and demand profiles, (2) to determine the relative impact on the same power plant knowing the high temperature and demand profiles, and (3) assessing the relative impact on the condensers with varied design parameters and cleaning schedules. *Ibrahim et al*.[8] presented a parametric study that illustrates the impact of the fouling factor of the seawater-cooled condenser in a range of 1.5–3.5 $cm^2\,K\,W^{-1}$, and the temperature in a range of 15–30 °C. *Zhang et al*.[9] proposed a novel method to calculate the effective thermal conductivity of particulate fouling based on the Image-Pro-Plus image processing and calculated its thermal conductivity using the finite element method.

The *artificial neural network* (ANN) technique has been used in many scientific domains, such as in solar energy[10,11] and in solubility of solid drugs.[12] The ANN was used by *Melzi et al*. to develop the predictive models to estimate the molecular diffusion coefficients of various gases

* Corresponding author: Mamaar Laidi, PhD
Email: maamarw@yahoo.fr; laidi.maamar@univ-medea.dz

at multiple pressures over a large field of temperatures.[13] They experimentally illustrated two optimisation objectives through developing two neural network models. The calculation of maximum flux as well as minimum resistance to fouling throughout ultra-filtration of industrial wastewater was anticipated by means of the genetic algorithm and assembled ANNs by *Soleimani et al*.[14] They provided a review consisting of three objectives on the thermal analysis of heat exchangers: (1) summarising the studies carried out by ANN, (2) comparing the network architectures, and (3) identifying the supplementary research boundaries and needs of ANN. In the work of *Mohanraj et al*.[15] ANN gave an exceptional alternative methodology for the thermal analysis of heat exchangers. From the experimental data, *Jradi et al*.[16] developed three accurate and reliable models of fouling phenomenon in three types of heat exchangers using three methods: Kern and Seaton model, Partial Least Squares model, and Artificial Neural Network model, in order to make a comparative study based on some statistical indices among these different models in regard to the modelling, and the losses prediction of heat exchangers performances due to the fouling phenomenon. The inputs to the ANN model used for the three types of exchangers were inlet and outlet temperatures, steam temperature, volume flow rate, density, and time. *Davoudi and Vaferi*[17] developed an ANN model for the estimation of the degree of fouling. The inputs for the network were density, surface temperature, fluid temperature, diameter of fluid passage, velocity of fluid, concentration of dissolved oxygen in fluid, and time. *Kashani et al*.[18] developed an ANN model to estimate the online monitoring and prediction of crude oil fouling behaviour for industrial shell and tube heat exchangers. The input data to the network were tube-side crude oil flow rate, tube-side inlet temperature, and shell-side inlet temperature. *Aminian and Shahhosseini*[19] employed an ANN model for developing a set of mathematical formulations in order to identify regions where there was less/no fouling for pre-heat exchangers of a crude oil by using input variables such as Reynolds number (Re), Prandtl number (Pr), and surface temperature.

Hence, the scientific contribution of this research is to predict the fouling resistance in heat exchanger-condenser (FR^*) using the ANN approach, and based on dimensionless inputs and output. To facilitate the use of the developed ANN model, MATLAB graphical interface was developed to facilitate the calculation for users.

Furthermore, a strategy will be developed to estimate the optimal operating conditions (inputs) from fouling resistance (FR^*) using *inverse artificial neural network* (ANNi).

2 Artificial neural networks approach

A neural network is an extremely parallel distributed processor that has a natural propensity for storing experiential knowledge and availing it for use.[20]

ANN is an adaptive non-linear statistical data modelling technique consisting of interconnected artificial neurons processing data in parallel. In this study, the multi-layer perceptron (MLP) network type was employed (Fig. 1), and the supervised learning process was used for the network parameters adjustment.

The input and output data were normalised within the range of [−1, 1] using a Mapminmax algorithm given by Eq. (1) that performs a normalisation of the maximum and minimum value of each row:[21]

$$y = \text{Mapminmax}(x) = \frac{(y_{max} - y_{min})(x - x_{min})}{(x_{max} - x_{min})} + y_{min} \qquad (1)$$

After examination of a considerable number of differently structured neural networks, the adequate ANN selected in this paper has a single hidden layer with seven neurons, and an output layer with one neuron. The hidden layer has a tansig transfer function. The output layer has a purelin transfer function. Typical structure of the ANN is shown in Fig. 1.

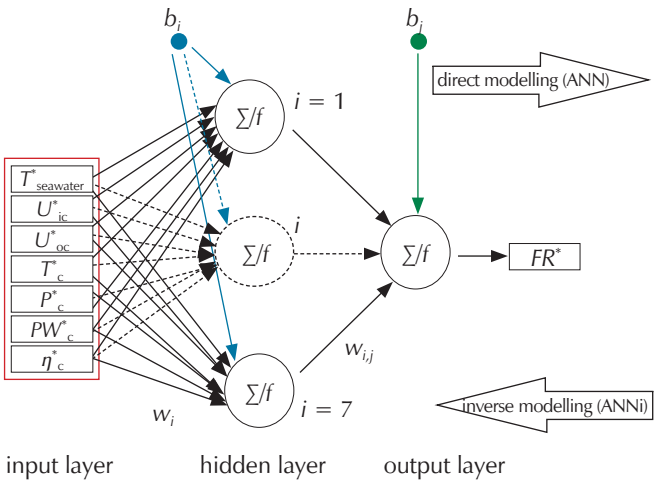

Fig. 1 – Structure of the constructed three-layer feed-forward back-propagation ANN to predict FR^*

3 Modelling procedure

3.1 Database collection

The experimental database regarding the fouling of condenser tubes cooling seawater of a pressurized water reactor nuclear power plant was collected from the literature.[8] Based on the effect of the environmental conditions and the change in fouling on the thermal performance of the condenser and the thermal efficiency of a nuclear power plant, the dimensional experimental inputs were transformed into dimensionless form. This base was transformed to dimensionless numbers including the different values of condenser cooling seawater temperature, inside overall heat transfer coefficient, outside overall heat transfer coefficient, condenser temperature, condenser pressure, output power, overall thermal efficiency, and the fouling resistance.

In this paper, a methodology was given for selecting ANN model to predict the fouling resistance of condenser. The objective of this paper was to select the best model. The methodology started with an extensive search in order to select a model with minimal complexity and optimal performance. The number of observed data used in the ANN was 600, which were divided into three sections: the training set (480 data), the test set (60 data), and the validation set (60 data). Training, test, and validation subsets of the ANN were obtained by selecting 80 % of the dataset as training, 10 % of the dataset as test, and 10 % of the dataset as validation subsets. A summary of the range of different variables is shown in Table 1.

Table 1 – Range of dimensionless variables[8]

Parameter	Unit	Min	Max
different values of dimensionless condenser cooling seawater temperature ($T^*_{seawater}$)	–	0.6	1.2
dimensionless inside overall heat transfer coefficient (U^*_{ic})	–	0.49459	0.85544
dimensionless outside overall heat transfer coefficient (U^*_{oc})	–	0.67473	0.86058
dimensionless condenser temperature (T^*_c)	–	1.04271	1.17221
dimensionless condenser pressure (P^*_c)	–	1.14258	1.44513
dimensionless output power(PW^*_c)	–	0.97831	0.99251
dimensionless overall thermal efficiency (η^*_c)	–	0.97738	0.99154
dimensionless fouling resistance (FR^*)	–	0.00015	0.00035

The difference between the observed and predicted values was filtered back through the system and used to adjust the connections between the layers, thus the performance improved. The root mean square error (RMSE) was the main criterion to evaluate the performance of ANN, which is defined as follows:[22,23]

$$\mathrm{RMSE} = \left[\frac{1}{n}\sum_{i=1}^{n}\left(y_i - y_i^{\mathrm{t}}\right)^2\right]^{\frac{1}{2}} \tag{2}$$

The statistical quality of the ANN for the three training, test, and validation sets was then evaluated using the coefficient of determination (R^2), relative absolute error (RAE), mean absolute percentage error (MAPE), mean square error (MSE), precision factor (A_f), bias factor (B_f), and acceptability criteria K and K'.

$$R^2 = 1 - \frac{\sum_{i=1}^{n}\left(y_i - y_i^{\mathrm{t}}\right)^2}{\sum_{i=1}^{n}\left(y_i - y_0\right)^2} \tag{3}$$

with:

$$y_0 = \frac{1}{n}\sum_{i=1}^{n}\left(y_i - y_i^{\mathrm{t}}\right) \tag{4}$$

$$\mathrm{MSE} = \frac{1}{n}\sum_{i=1}^{n}\left(y_i - y_i^{\mathrm{t}}\right)^2 \tag{5}$$

$$\mathrm{RAE}_i(\%) = \left|\frac{\left|y_i\right| - \left|y_i^{\mathrm{t}}\right|}{y_i}\right| \cdot 100 \tag{6}$$

$$\mathrm{MAPE}(\%) = \frac{1}{n}\sum_{i=1}^{n}\mathrm{RAE}_i \tag{7}$$

Ross[24] proposed two different indices for determination of the model performance. The bias factor B_f (Eq. (8)) is a measure of overall agreement between the predicted and the observed values. It will indicate whether and to what extent the forecasts are above or below the equivalence line. A perfect agreement between the observed and the predicted values would give a $B_f = 1$. ($B_f = 0.90 – 1.05$ means good model).

The accuracy factor value, A_f (Eq. (9)), will always be equal to or greater than one as all variances are positive.

$$B_f = 10^{\frac{1}{n}\sum_{i=1}^{n}\log\frac{y_i^{\mathrm{t}}}{y_i}} \tag{8}$$

$$A_f = 10^{\frac{1}{n}\sum_{i=1}^{n}\left|\log\frac{y_i^{\mathrm{t}}}{y_i}\right|} \tag{9}$$

In addition, to ensure greater validity of the developed models, some statistical criteria were used as follows:

$$K = \frac{\sum y_i^{\mathrm{t}} y_i}{\sum\left(y_i^{\mathrm{t}}\right)^2} \tag{10}$$

$$K' = \frac{\sum y_i^{\mathrm{t}} y_i}{\sum\left(y_i\right)^2} \tag{11}$$

where $0.85 \leq K \leq 1.15$; $0.85 \leq K' \leq 1.15$ was acceptability criteria.

y_i represents the i^{th} trained test or validation output value, and y_i^{t} represents the corresponding target value, with n being the number of input vectors.

3.2 Modelling with neural networks

The objective of this work was to build a model to predict the resistance of fouling in heat exchanger-condenser. ANN was chosen as the main modelling tool to perform the task.

Different values of dimensionless condenser cooling seawater temperature, dimensionless inside overall heat transfer coefficient, dimensionless outside overall heat transfer coefficient, dimensionless condenser temperature, dimensionless condenser pressure, dimensionless output power, and dimensionless overall thermal efficiency were input

Table 2 – Structure of the 1st ANN

Type of network	No. of neurons in the hidden layer	Transfer function in the hidden layer	Transfer function in the output layer	Learning algorithm	No. of iterations
MLP 2 layers	7	tangential sigmoid	identity	Levenberg–Marquardt	631

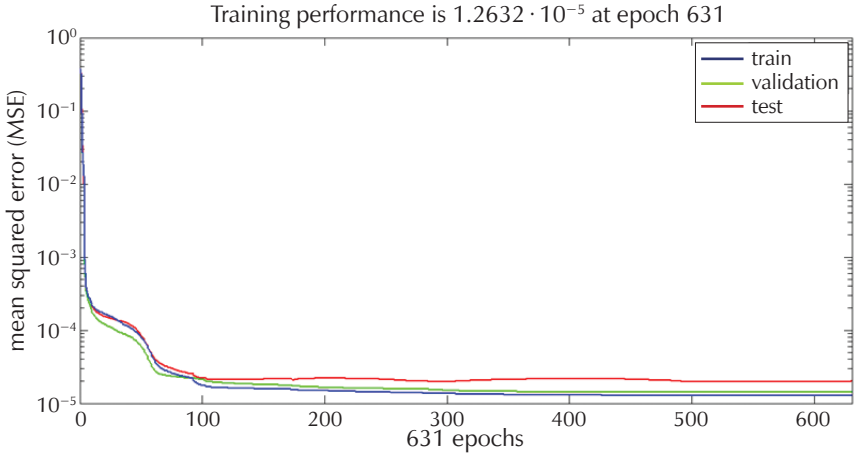

Fig. 2 – Training with TRAINLM function diagram

Table 3 – Statistical performance of the ANN model

	RAE_{min}/%	RAE_{max}/%	MAPE/%	MSE	RMSE	A_f	B_f	k	k'	R^2
training	$8.3227 \cdot 10^{-4}$	0.4781	0.1211	$1.3051 \cdot 10^{-13}$	$3.6127 \cdot 10^{-7}$	1	1	1.0000	1.0000	0.99996
testing	$2.6989 \cdot 10^{-5}$	0.5952	0.1393	$2.3354 \cdot 10^{-13}$	$4.8326 \cdot 10^{-7}$	1	1	0.9995	1.0005	0.99993
validation	0.0055	0.3146	0.1295	$1.3386 \cdot 10^{-13}$	$3.6588 \cdot 10^{-7}$	1	1	0.9998	1.0002	0.99996
all	$2.6989 \cdot 10^{-5}$	0.5952	0.1238	$1.4116 \cdot 10^{-13}$	$3.7572 \cdot 10^{-7}$	1	1	0.9999	1.0001	0.99996

arguments for network (independent variables), while dimensionless fouling resistance was a target argument (dependent variable). The structure of the database used for the model is shown in Table 2 and Fig. 2.

In this part, listed are all the important stages that led to the solution of the optimisation of neural networks. The following parameters were examined and optimised during the development of the best network for prediction of fouling resistance: selection of input and output data, possible transfer functions, learning mode, stopping criteria, learning algorithm, normalisation technique, number of hidden layers, number of hidden nodes, and performance evaluation measures. The results are summarised in Table 3.

Observed and predicted (dimensionless fouling resistance) breakthrough curves shown in Fig. 3 indicate that the ANN describes the experimental data well.

4 Results and discussion

4.1 Neural networks

A learning algorithm is defined as a procedure of adjusting the coefficients (weight and bias) of a network to minimise an error function (usually quadratic) between the outputs of the network for a given set of inputs and the correct outputs (already known). If nonlinearities are used, the gradient of the error function can be calculated by the conventional backpropagation procedure.[25] To establish the best algorithm of backpropagation learning, a set of fourteen backpropagation algorithms were studied. In addition, thirty neurons were used in the hidden layer for all backpropagation algorithms. Table 4 presents a comparison of different retro-propagation training algorithms. In the present study, the Levenberg–Marquardt algorithm was considered as the learning algorithm because it might have a smaller maximum relative absolute error (RAE_{max}) compared to the other learning algorithms.

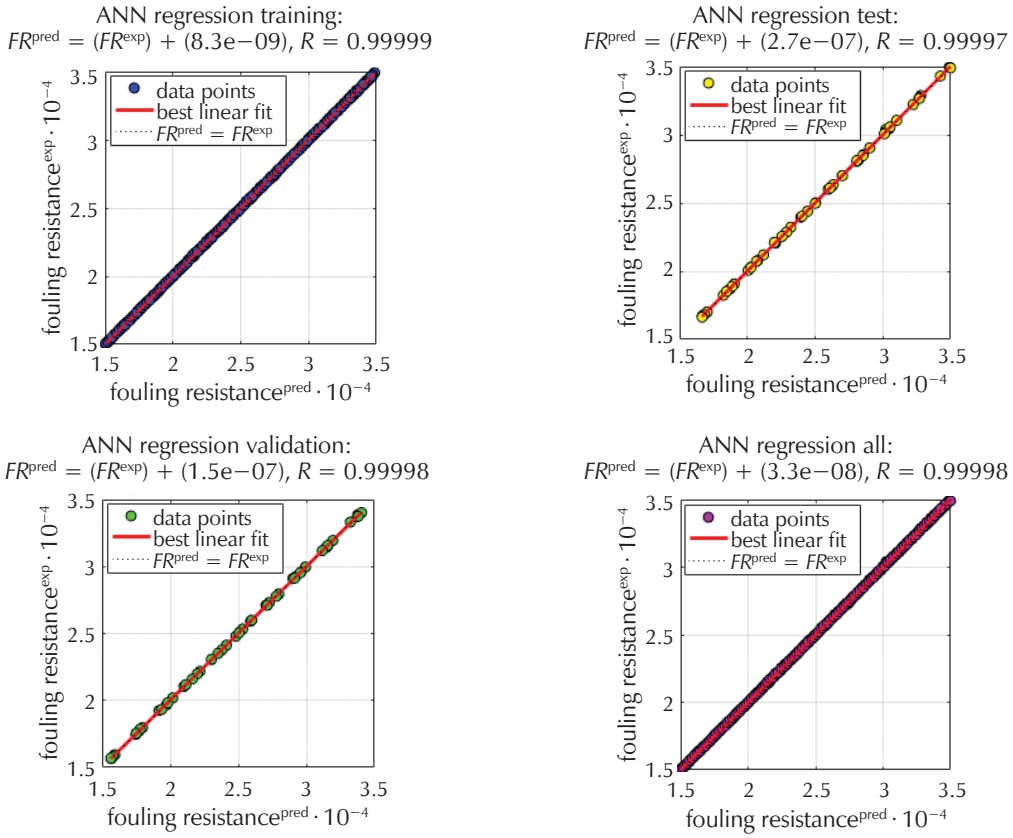

Fig. 3 – Plot between experimental and ANN predicted dimensionless fouling resistance for training data set, for testing data set, for validation data set, and for all data set

Table 4 – Comparison of 14 back propagation algorithms with 30 neurons in the hidden layer

Backpropagation algorithm	Function	Relative absolute error (RAE_{max})/%	Number of epochs	R^2	Best linear fit
Levenberg–Marquardt backpropagation	**trainlm**	**0.314**	**1000**	**0.99996**	**$Y = 1X+1.5 \cdot 10^{-7}$**
Bayesian regularization backpropagation	trainbr	0.317	1000	0.99996	$Y = 1X-4.6 \cdot 10^{-10}$
Powell–Beale conjugate gradient backpropagation	traincgb	0.354	1000	0.99985	$Y = 1X+8.9 \cdot 10^{-8}$
Fletcher–Reeves conjugate gradient backpropagation	traincgf	0.989	1000	0.99984	$Y = 1X+4.6 \cdot 10^{-8}$
Polak-Ribiére conjugate gradient backpropagation	traincgp	1.142	1000	0.99982	$Y = 1X+1.9 \cdot 10^{-7}$
Scaled conjugate gradient backpropagation	trainscg	0.954	1000	0.99987	$Y = 1X+1.9 \cdot 10^{-8}$
Batch gradient descent	traingd	2.840	1000	0.99739	$Y = 0.99X+1.4 \cdot 10^{-6}$
Gradient descent with adaptive learning rate backpropagation	traingda	2.604	1000	0.99831	$Y = 1X+8.8 \cdot 10^{-7}$
Batch gradient descent with momentum	traingdm	3.085	1000	0.99684	$Y = 0.99X+1.5 \cdot 10^{-6}$
Variable learning rate backpropagation	traingdx	2.589	1000	0.99884	$Y = 1X+6.3 \cdot 10^{-7}$
One step secant backpropagation	trainoss	1.068	1000	0.99982	$Y = 1X+1.2 \cdot 10^{-7}$
Resilient backpropagation	trainrp	0.759	1000	0.99980	$Y = 1X+4.7 \cdot 10^{-8}$
BFGS Quasi-Newton backpropagation	trainbfg	0.341	1000	0.99997	$Y = 1X-2.5 \cdot 10^{-10}$
Random order incremental training	trainr	2.001	1000	0.99938	$Y = 0.99X+1 \cdot 10^{-6}$

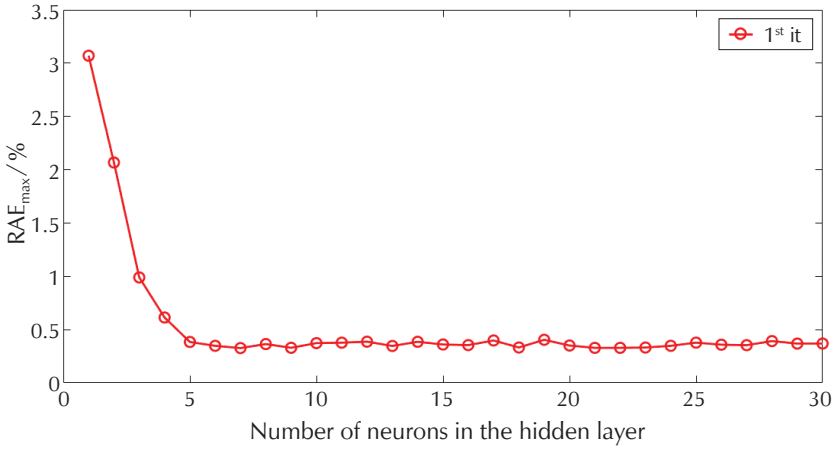

Fig. 4 – Effect of the number of neurons in the hidden layer on the relative absolute error of the neural network

However, the performance of the ANN model was statistically measured by RAE_{max} and R^2 according to Eq. (3), which was calculated using the experimental values and network predictions. As a result, RAE_{max} was used as an error function that measures network performance. The network RAE_{max} and maximum R^2 were selected as the best ANN model.

To obtain the optimal number of neurons in the hidden layer, a series of topologies were used, using the scaled conjugate gradient algorithm such as the number of neurons ranging from 1 to 30 (Fig. 4) in order to maximise RAE_{max} by looking for a set of weights and connection bias that cause the ANN to produce outputs equal or close to the target values.

To approximate the actual data points, a statistical measure that gives the quality and efficiency of the fit of the regression line of a model was verified by R^2. R^2 of 0.99996 means that the regression line matches the data.

The forecasts of the results by ANN with respect to the experimental results for training, test, and validation data sets are plotted in Fig. 5 for the fouling resistance. The performance of the selected networks {7-7-1} is described in Fig. 5. The ANN was well formed because R^2 was greater than 0.9999 for the forecast network.

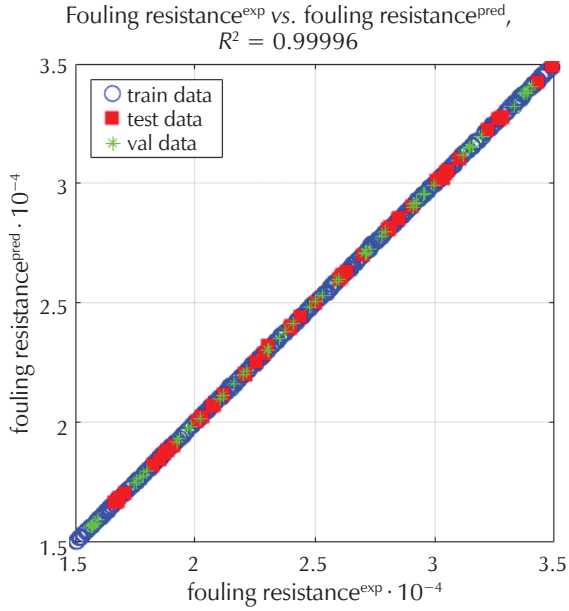

Fig. 5 – Plot between experimental and neural network prediction of fouling resistance

4.2 Sensitivity analysis

In order to study the effects of the selected input parameters on the planned outputs, a sensitivity study was performed, where the model that was chosen to study had 7 inputs, 1 output, and 7 neurons in its hidden layer. The Min-Max method was used as a normalisation technique and the Levenberg–Marquardt as the learning algorithm. Once the network had been trained and optimised, weights matrix was generated (Table 5).

In order to evaluate the relative importance of the input variables, the weights matrix was exploited in Eq. (12) proposed by *Garson*:[26]

$$I_J = \frac{\sum_{m=1}^{m=N_h}\left(\left(\left|w_{j_m}^{i_n}\right| \Big/ \sum_{k=1}^{N_i}\left|w_{k_m}^{i_h}\right|\right)\times\left|w_{m_n}^{h_o}\right|\right)}{\sum_{k=1}^{k=N_i}\left\{\sum_{m=1}^{m=N_h}\left(\left(\left|w_{j_m}^{i_n}\right| \Big/ \sum_{k=1}^{N_i}\left|w_{k_m}^{i_h}\right|\right)\times\left|w_{m_n}^{h_o}\right|\right)\right\}} \qquad (12)$$

where I_j represents the relative importance of the j^{th} input variable on the output variable, N_i and N_h are the set of input and hidden neurons, respectively, W is the connection weights, the exponents 'i', 'h' and 'o' refer to the input, hidden and output layers, respectively, and 'k', 'm' and 'n' refer to the input, hidden, and output neurons, respectively. Note that the numerator in Eq. (12) describes the sum of the products of the absolute weights for each entry. However, the denominator in Eq. (12) represents the sum of all the weights feeding the hidden unit, taking the absolute values.[26] A summary of the results obtained is presented in

Fig. 6, where it was found that all the input variables had strong effect on the estimation of the fouling resistance.

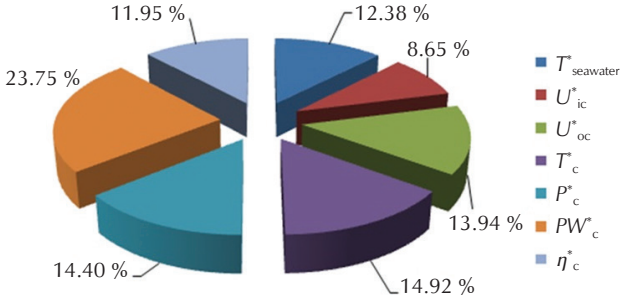

Fig. 6 – Relative importance (%) of input variables on the value of the calculated fouling resistance

4.3 Interface for dimensionless fouling resistance

Our model based on the mathematical non-linear formula of the optimised neural network (ANN) is presented by Eq. (13) linking the inputs to the output (Table 2).

$$FR^* = \sum_{n=1}^{n}\left[w_{ij(1.n)} \left(\frac{2}{1+\exp\left(-2\left(\left(\sum_{m=1}^{m} i(n.m)\ln_{(m)}\right)+b_{i(n)}\right)\right)} - 1 \right)\right] + b_j \quad (13)$$

After having optimised the neural network model, a computer program was developed in MATLAB (Fig. 7). This allows the user to have all the inputs needed to run the model in order to calculate the fouling resistance in the condenser. The interface was designed to provide more flexibility in the use of ANN model for quick and easy calculation of fouling resistance.

4.4 Optimal performance by means of ANNi

According to the ANN model, developed was a method of estimating input parameters that influence the resistance of fouling when the input parameters are well known.[12,27,28]

Table 5 gives the obtained parameters (w_i, w_{ij}, b_i, and b_j) of the best fit for seven neurons in the hidden layer. These parameters are used in the proposed model to simulate the FR^* value.

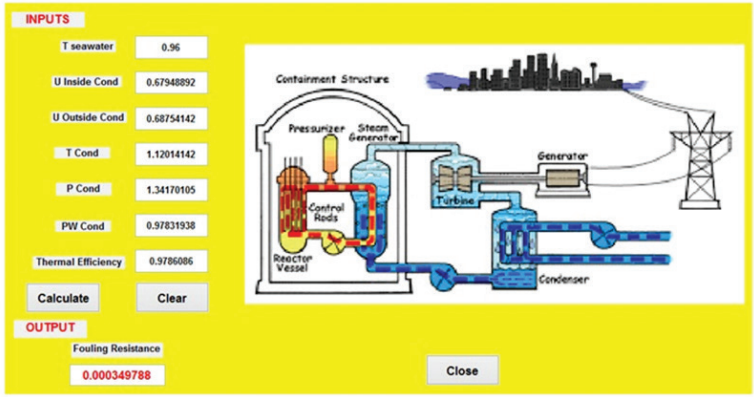

Fig. 7 – MATLAB interface for dimensionless fouling resistance

Table 5 – Statistical parameters obtained for the ANN model

No. of neurons	w_1							Bias	w_2	Bias
	$T^*_{seawater}$	U^*_{ic}	U^*_{oc}	T^*_c	P^*_c	PW^*_c	η^*_c	1	FR^*	2
1	0.500326	−0.969916	1.198230	0.712472	−2.217929	−0.598790	−0.462936	−1.072256	−0.386981	
2	−0.459379	0.476224	1.087681	0.718236	0.505942	1.242267	−0.362146	−2.384026	−0.138044	
3	−1.096048	1.655369	−1.384254	−0.949099	−0.624925	0.343710	−0.243276	0.895478	−1.982093	
4	1.537030	−4.655751	2.070056	0.953992	0.937874	0.074150	1.044117	0.176574	−1.911302	0.22485
5	0.007095	2.364086	0.371170	0.270999	0.265573	−0.15699	−0.302598	−0.324478	−0.613290	
6	0.551937	−0.085535	0.465512	0.321671	−0.687249	−0.163053	0.021205	0.793517	−0.960898	
7	0.204665	−1.372054	0.482392	0.34565	−0.615597	−0.187586	−0.149514	0.868911	1.084011	

w_1: weight matrix between the input and hidden layers.
w_2: weight matrix between the hidden and output layers.

A general network is constituted by transfer function (tansig and purelin). Then, the output is given as function of inputs Eq. (14), where n is the number of neurons in the hidden layer ($n = 7$), m is the number of the input ($m = 7$), w is the weight, and b is the bias.

Eq. (13) can be expressed as:

$$FR^* = b_j - \sum_n w_{ij(1.n)} + \sum_s \left[\frac{2w_{ij(i.n)}}{1+\exp\left(-2\left(\left(\sum_m w_{i(n.m)} \mathrm{In}_{(m)}\right) + b_{i(n)}\right)\right)} \right] \quad (14)$$

At this step, the function was obtained that had to be minimised at zero to obtain optimal input parameters (n) $\mathrm{In}_{(m=x)}$:

$$\mathrm{Fun}\left(\mathrm{In}_{(m)}\right) = b_j - \sum_n w_{ij(i.n)} + \\ + \sum_n \left[\frac{2w_{ij(i.n)}}{1+\exp\left(-2\left(w_{i(n.m)}\mathrm{In}_{(x)} + \sum_{m\neq x} w_{i(n.m)}\mathrm{In}_{(m)} + b_{i(n)}\right)\right)} \right] \quad (15)$$

where x are the different values of dimensionless condenser cooling seawater temperature value to be computed. The proposed ANN model had seven neurons in the hidden layer. It was therefore essential to apply an optimisation method.[29,30]

Optimised input parameter was established using Nelder-Mead simplex algorithms under the different conditions to prove the feasibility of using ANNi. A test was done with different data to optimise one of the inputs – for instance, different values of dimensionless condenser cooling seawater temperature (T^*_{seawater}) on the one hand, and on the other hand, the simulated parameters were compared to the experimental data in order to check the accuracy of ANNi at way of the error given in the Eq. (16).

$$\mathrm{error} = \frac{|\exp - \mathrm{sim}|}{\exp} \cdot 100 \quad (16)$$

Case1. A group of parameters was provided for fouling resistance predicted process with $k = 1$, $n = 7$, and $m = 7$. The input value (for example T^*_{seawater}) can be calculated through ANNi. The experimental conditions for this test, for a required output value $FR^* = 0.00015$, with input values: $U^*_{\mathrm{ic}} = 0.855440$, $U^*_{\mathrm{oc}} = 0.860584$, $T^*_{\mathrm{c}} = 1.07401318$, $P^*_{\mathrm{c}} = 1.161460$, $PW^*_{\mathrm{c}} = 0.991597$, $\eta^*_{\mathrm{c}} = 0.991542$, by minimising the nonlinear function given in Eq. (17).

$$F = -A + \frac{2w_{ij(1.1)}}{1+\exp\left(x_1 + 2w_{i(1.7)}T^*_{\mathrm{seawater}}\right)} + \\ + \frac{2w_{ij(1.2)}}{1+\exp\left(x_2 + 2w_{i(2.7)}T^*_{\mathrm{seawater}}\right)} + \\ + \frac{2w_{ij(1.3)}}{1+\exp\left(x_3 + 2w_{i(3.7)}T^*_{\mathrm{seawater}}\right)} + \\ + \frac{2w_{ij(1.4)}}{1+\exp\left(x_4 + 2w_{i(4.7)}T^*_{\mathrm{seawater}}\right)} + \\ + \frac{2w_{ij(1.5)}}{1+\exp\left(x_5 + 2w_{i(5.7)}T^*_{\mathrm{seawater}}\right)} + \\ + \frac{2w_{ij(1.6)}}{1+\exp\left(x_6 + 2w_{i(6.7)}T^*_{\mathrm{seawater}}\right)} + \\ + \frac{2w_{ij(1.7)}}{1+\exp\left(x_7 + 2w_{i(7.7)}T^*_{\mathrm{seawater}}\right)} \quad (17)$$

where

$$A = FR^* - b_j + w_{ij(1.1)} + w_{ij(1.2)} + w_{ij(1.3)} + w_{ij(1.4)} + w_{ij(1.5)} + w_{ij(1.6)} + w_{ij(1.7)} \quad (18)$$

$$x_1 = -2\left(w_{i(1.2)}v_2 + w_{i(1.3)}v_3 + w_{i(1.4)}v_4 + w_{i(1.5)}v_5 + w_{i(1.6)}v_6 + w_{i(1.7)}v_7 + b_1\right) \quad (19)$$

$$x_2 = -\left(w_{i(2.2)}v_2 + w_{i(2.3)}v_3 + w_{i(2.4)}v_4 + w_{i(2.5)}v_5 + w_{i(2.6)}v_6 + w_{i(2.7)}v_7 + b_2\right) \quad (20)$$

$$x_3 = -2\left(w_{i(3.2)}v_2 + w_{i(3.3)}v_3 + w_{i(3.4)}v_4 + w_{i(3.5)}v_5 + w_{i(3.6)}v_6 + w_{i(3.7)}v_7 + b_3\right) \quad (21)$$

$$x_4 = -2\left(w_{i(4.2)}v_2 + w_{i(4.3)}v_3 + w_{i(4.4)}v_4 + w_{i(4.5)}v_5 + w_{i(4.6)}v_6 + w_{i(4.7)}v_7 + b_4\right) \quad (22)$$

$$x_5 = -2\left(w_{i(5.2)}v_2 + w_{i(5.3)}v_3 + w_{i(5.4)}v_4 + w_{i(5.5)}v_5 + w_{i(5.6)}v_6 + w_{i(5.7)}v_7 + b_5\right) \quad (23)$$

$$x_6 = -2\left(w_{i(6.2)}v_2 + w_{i(6.3)}v_3 + w_{i(6.4)}v_4 + w_{i(6.5)}v_5 + w_{i(6.6)}v_6 + w_{i(6.7)}v_7 + b_6\right) \quad (24)$$

$$x_7 = -2\left(w_{i(7.2)}v_2 + w_{i(7.3)}v_3 + w_{i(7.4)}v_4 + w_{i(7.5)}v_5 + w_{i(7.6)}v_6 + w_{i(7.7)}v_7 + b_7\right) \quad (25)$$

v_1: Different values of dimensionless condenser cooling seawater temperature;
v_2: Inside overall dimensionless heat transfer coefficient;
v_3: Outside overall dimensionless heat transfer coefficient;
v_4: Dimensionless condenser temperature;
v_5: Dimensionless condenser pressure;
v_6: Dimensionless output power;
v_7: Overall dimensionless thermal efficiency.

With weights and biases, the optimum T^*_{seawater} of the process can be calculated for the required output, using MATLAB software with the optimisation Toolbox.[31] The outcome value (T^*_{seawater}) simulated by ANNi was 0.6. Furthermore, using Eq. (17), the calculated value had an error of 0 % regarding the experimental result (Table 6).

Table 6 – Error between experimental inputs and those calculated by ANNi

ANNi inputs	Experimental	Calculated	error/%
Input 1	0.6000	0.6000	0.00
Input 2	0.8554	0.8528	0.30
Input 3	0.8605	0.8605	0.00
Input 4	1.0740	1.0740	0.00
Input 5	1.1615	1.1615	0.00
Input 6	0.9916	0.9908	0.07
Input 7	0.9915	0.9985	0.30

5 Comparison with other models

In order to evaluate the importance of the obtained results, they were compared with similar studies cited in the Introduction,[16–19] especially with the models that had the same or mostly the same inputs as we used. It was found that, in most models, the goal was to predict the fouling in heat exchangers. The results obtained from these mentioned models and results in this work are collected in Table 7.

6 Conclusion

The ANN modelling method has many advantages, such as speed, adaptability, generalisation and simplicity, making it an interesting choice for the modelling of nonlinear complex systems (fouling of heat exchanger-condenser).

During the training process, several configurations of neural networks were used. It started with the use of 14 training algorithms by observing the effect of each of them on the network performance. Therefore, the top three of them (*trainlm*, *trainbr*, *trainbfg*) were chosen, and improvement of their performance was attempted by using one normalisation technique. Among the three obtained networks, the best predicting network was selected, which had also been tested with one hidden layer and several hidden nodes. It was found that one hidden layer with 7 neurons can provide a better prediction.

Our model was developed by MLP back-propagation architecture with direct action with the Levenberg–Marquardt training algorithm. The results confirm that the MLP neural networks are competent enough to predict fouling resistance when using the heat exchanger-condenser operating conditions as inputs.

It was observed that the network with a hidden layer of {7-7-1} gave a correlation coefficient greater than 0.9999 with a small error (RMSE = $3.6588 \cdot 10^{-7}$) for the whole database, meaning that the neural network was well formed. The ANN is an adequate interpolation tool for the non-linear behaviour of FR^* for all the operating conditions mentioned above, in which an excellent prediction was obtained. Based on the sensitivity analysis, it was found that all the input variables had a significant effect on the estimation of fouling resistance. In addition, based on the model, a methodology was developed to estimate the optimal operating conditions from ANNi when necessary to obtain an optimal result for the known inputs for the required fouling resistance FR^* by applying the Nelder-Mead simplex optimisation method. Nevertheless, the mathematical calculation of ANNi was carried out in Case 1.

All ANN inputs were estimated using ANNi with an average relative deviation not exceeding 0.095 %. By comparing these results to other studies in the same context, it may be concluded that our model gave better performance compared to many other models.

ACKNOWLEDGEMENTS

The authors are grateful to the Laboratory of Biomaterials and Transport Phenomena (LBMPT) of the University of Médéa of the University Training Research Project (PRFU) of the Directorate-General for Scientific Research and Technological Development (DGRSDT) under the Algerian Ministry of Education and Scientific Research (MESRS) for

Table 7 – Results of current model *vs.* various similar models

Name of model	Fouling in heat exchangers										
	RAE_{min}/%	RAE_{max}/%	MAPE/%	MSE	RMSE	A_f	B_f	k	k'	R	R^2
Current model	0.0055	0.3146	0.1295	$1.338 \cdot 10^{-13}$	$3.6588 \cdot 10^{-7}$	1	1	0.9998	1.0002	0.99998	0.99996
Jradi et al.:[16]											
– stainless-steel tubular heat exchanger	–	–	0.065	$2.168 \cdot 10^{-11}$	$4.656 \cdot 10^{-6}$	–	–	–	–	0.994	–
– graphite blocks heat exchanger (A)	–	–	0.048	$1.811 \cdot 10^{-11}$	$4.2561 \cdot 10^{-6}$	–	–	–	–	0.995	–
– graphite blocks heat exchanger (B)	–	–	0.046	$6.577 \cdot 10^{-11}$	$8.110 \cdot 10^{-6}$	–	–	–	–	0.993	–
Davoudi and Vaferi[17]	–	–	5.42	0.0013	0.0355	–	–	–	–	–	0.977819
Kashani et al.[18]	–	8	–	–	–	–	–	–	–	–	–
Aminian and Shahhosseini[19]	–	–	15.83	–	–	–	–	–	–	–	–

the financial support provided. The authors also express their gratitude for useful and interesting discussions with researchers at the Birine Nuclear Research Center (CRNB).

List of abbreviations and symbols

AE – absolute error

A_f – precision factor

ANN – artificial neural network

ANNi – inverse artificial neural network

B – bias of artificial neural model

B_f – bias factor

FR^* – dimensionless fouling resistance ($FR^* = \frac{FR_{cexp}}{FR_\infty} = \frac{FR_{exp}}{1}$)

I – relative importance

K, K' – acceptability criteria

LM – Levenberg–Marquardt

MAPE – mean absolute percentage error

MLP – multi-layer perceptron

MSE – mean square error

P^*_c – dimensionless condenser pressure ($P^*_c = \frac{P_{cexp}}{P_0}$), $P_0 = 0.04569$

PW^*_c – dimensionless output power ($PW^*_c = \frac{PW_{cexp}}{PW_0}$), $PW_0 = 999644.52$

R – correlation coefficient

RAE_{max} – maximum relative absolute error

RAE_{min} – minimum relative absolute error

RMSE – root mean square error

R^2 – determination coefficient

T^*_c – dimensionless condenser temperature ($T^*_c = \frac{T_{cexp}}{T_0}$), $T_0 = 31.6268$

$T^*_{seawater}$ – different values of dimensionless condenser cooling seawater temperature ($T^*_{seawater} = \frac{T_{seawater\ exp}}{25}$)

U^*_{ic} – inside overall dimensionless heat transfer coefficient ($U^*_{ic} = \frac{U_{icexp}}{U_0}$), $U_0 = 1236.45$

U^*_{oc} – outside overall dimensionless heat transfer coefficient ($U^*_{oc} = \frac{U_{ocexp}}{U_0}$), $U_0 = 1178.502$

W – input layer–hidden layer synaptic weights of artificial neural model

η^*_c – dimensionless overall thermal efficiency ($\eta^*_c = \frac{\eta_{cexp}}{\eta_0}$), $\eta_0 = 37.117$

References
Literatura

1. *E. Eguía, T. F. Vidart, J. A. Bezanilla, J. J. Amieva, P. M. Otero, M. A. Giron, B. Río-Calonge, M. Ruiz*, Elimination of biofouling in heat exchangers-condensers by different chemical methods, WIT Trans. Built Environ. **39** (1970), doi: https://doi.org/10.2495/MAR980281.
2. *S. M. Zubair, A. K. Sheikh, M. Younas, M. O. Budair*, A risk based heat exchanger analysis subject to fouling: Part I: Performance evaluation, Energy **25** (2000) 427–443, doi: https://doi.org/10.1016/S0360-5442(99)00080-8.
3. *J. F. Casanueva, J. Sánchez, J. L. García-Morales, T. Casanueva-Robles, J. A. López, J. R. Portela, E. Nebot, D. Sales*, Portable pilot plant for evaluating marine biofouling growth and control in heat exchangers-condensers, Water Sci. Technol. **47** (2003) 99–104, doi: https://doi.org/10.2166/wst.2003.0291.
4. *B. A. Qureshi, S. M. Zubair*, The impact of fouling on performance evaluation of evaporative coolers and condensers, Int. J. Energy Res. **29** (2005) 1313–1330, doi: https://doi.org/10.1002/er.1120.
5. *A. Durmayaz, O. S. Sogut*, Influence of cooling water temperature on the efficiency of a pressurized-water reactor nuclear-power plant, Int. J. Energy Res. **30** (2006) 799–810, doi: https://doi.org/10.1002/er.1186.
6. *E. Nebot, J. F. Casanueva, T. Casanueva, D. Sales*, Model for fouling deposition on power plant steam condensers cooled with seawater: Effect of water velocity and tube material, Int. J. Heat Mass Trans. **50** (2007) 3351–3358, doi: https://doi.org/10.1016/j.ijheatmasstransfer.2007.01.022.
7. *M. E. Walker, I. Safari, R. B. Theregowda, M. K. Hsieh, J. Abbasian, H. Arastoopour, D. A. Dzombak, D. C. Miller*, Economic impact of condenser fouling in existing thermoelectric power plants, Energy **44** (2012) 429–437, doi: https://doi.org/10.1016/j.energy.2012.06.010.
8. *S. M. Ibrahim, S. I. Attia*, The influence of condenser cooling seawater fouling on the thermal performance of a nuclear power plant, Ann. Nucl. Energy **76** (2015) 421–430, doi: https://doi.org/10.1016/j.anucene.2014.10.018.
9. *Z. B. Zhang, Y. Liu, L. H. Cao*, A novel method for calculating effective thermal conductivity of particulate fouling, Therm. Sci. (2019) 308–308, doi: https://doi.org/10.2298/TSCI190308308Z.
10. *A. Rezrazi, S. Hanini, M. Laidi*, An optimisation methodology of artificial neural network models for predicting solar radiation: a case study, Theoret. Appl. Climatol. **123** (2016)769–783, doi: https://doi.org/10.1007/s00704-015-1398-x.
11. *M. Laidi, S. Hanini*, Optimal solar COP prediction of a solar-assisted adsorption refrigeration system working with activated carbon/methanol as working pairs using direct and inverse artificial neural network, Int. J. Refrig. **36** (2013) 247–257, doi: https://doi.org/10.1016/j.ijrefrig.2012.09.016.
12. *A. Abdallahelhadj, M. Laidi, C. Si-Moussa, S. Hanini*, Novel approach for estimating solubility of solid drugs in supercritical carbon dioxide and critical properties using direct and inverse artificial neural network (ANN), Neur. Comput. Appl. **28** (2015) 87–99, doi: https://doi.org/10.1007/s00521-015-2038-1.
13. *N. Melzi, L. Khaouane, Y. Ammi, S. Hanini, M. Laidi, H. Zentou*, Comparative Study of Predicting the Molecular Diffu-

sion Coefficient for Polar and Non-polar Binary Gas Using Neural Networks and Multiple Linear Regressions, Kem. Ind. **68** (2019) 573–582, doi: https://doi.org/10.15255/KUI.2019.010.

14. *R. Soleimani, N. A. Shoushtari, B. Mirza, A. Salahi*, Experimental investigation, modeling and optimization of membrane separation using artificial neural network and multi-objective optimization using genetic algorithm, Chem. Eng. Res. Des. **91** (2013) 883903, doi: https://doi.org/10.1016/j.cherd.2012.08.004.
15. *M. Mohanraj, S. Jayaraj, C. Muraleedharan*, Applications of artificial neural networks for thermal analysis of heat exchangers– A review, Int. J. Therm. Sci. **90** (2015) 150–172, doi: https://doi.org/10.1016/j.ijthermalsci.2014.11.030.
16. *R. Jradi, C. Marvillet, M. R. Jeday*, Modeling and comparative study of heat exchangers fouling in phosphoric acid concentration plant using experimental data, Heat Mass Transf. **56** (2020) 1–14, doi: https://doi.org/10.1007/s00231-020-02888-9.
17. *E. Davoudi, B. Vaferi*, Applying artificial neural networks for systematic estimation of degree of fouling in heat exchangers, Chem. Eng. Res. Des. **130** (2018) 138153, doi: https://doi.org/10.1016/j.cherd.2017.12.017.
18. *M. N. Kashani, J. Aminian, S. Shahhosseini, M. Farrokhi*, Dynamic crude oil fouling prediction in industrial preheaters using optimized ANN based moving window technique, Chem. Eng. Res. Des. **90** (2012) 938–949, doi: https://doi.org/10.1016/j.cherd.2011.10.013.
19. *J. Aminian, S. Shahhosseini*, Neuro-based formulation to predict fouling threshold in crudepreheaters, Int. Commun. Heat Mass Transf. **36** (2009) 525–531, doi: https://doi.org/10.1016/j.icheatmasstransfer.2009.01.020.
20. *A. Nigrin*, Neural networks for pattern recognition, 1993, MIT press.
21. *H. Demuth, M. Beale*, Matlab neural network toolbox user's guide version 6, 2009, The MathWorks Inc.
22. *B. Mohamedi, S. Hanini, A. Ararem, N. Mellel*, Simulation of nucleate boiling under ANSYS-FLUENT code by using RPI model coupling with artificial neural networks, Nucl. Sci. Tech. **26** (2015) 40601–040601, doi: https://doi.org/10.13538/j.1001-8042/nst.26.040601.
23. *A. Ararem, A. Bouzidi, B. Mohamedi, O. Bouras*, Modeling of fixed-bed adsorption of Cs^{+} and Sr^{2+} onto clay–iron oxide composite using artificial neural network and constant–pattern wave approach, J. Radioanal. Nucl. Chem. **301** (2014) 881–887, doi: https://doi.org/10.1007/s10967-014-3200-4.
24. *T. Ross*, Indices for performance evaluation of predictive models in food microbiology, J. Appl. Bacterial. **81** (1996) 501–508, doi: https://doi.org/10.1111/j.1365-2672.1996.tb03539.x.
25. *D. E. Rumelhart, G. E. Hinton, R. J. Williams*, Learning internal representations by error propagation (No. ICS-8506), California Univ San Diego La Jolla Inst for Cognitive Science, 1985.
26. *D. G. Garson*, Interpreting neural network connection weights (1991) 47–51.
27. *Y. E. Hamzaoui, J. A. Hernández, S. Silva-Martínez, A. Bassam, A. Álvarez, C. Lizama-Bahena*, Optimal performance of COD removal during aqueous treatment of alazine and gesaprim commercial herbicides by direct and inverse neural network, Desalination **277** (2011) 325–337, doi: https://doi.org/10.1016/j.desal.2011.04.060.
28. *N. Hattab, M. Motelica-Heino*, Application of an inverse neural network model for the identification of optimal amendment to reduce copper toxicity in phytoremediated contaminated soils, J. Geochem. Explor. **136** (2014) 14–23, doi: https://doi.org/10.1016/j.gexplo.2013.09.002.
29. *J. A. Hernández*, Optimum operating conditions for heat and mass transfer in foodstuffs drying by means of neural network inverse, Food Control **20** (2009) 435–438, doi: https://doi.org/10.1016/j.foodcont.2008.07.005.
30. *O. Cortés, G. Urquiza, J. A. Hernández*, Optimization of operating conditions for compressor performance by means of neural network inverse, Appl. Energy **86** (2009) 2487–2493, doi: https://doi.org/10.1016/j.apenergy.2009.03.001.
31. *H. Demuth, M. Beale*, MATLAB: The Language of Technical Computing; Neutral Network Toolbox; User's Guide; Version 3, 1998, MathWorks.

SAŽETAK

Doprinos modeliranju otpora prljanja u izmjenjivaču topline-kondenzatoru izravnom i inverznom umjetnom neuronskom mrežom

Ahmed Benyekhlef,[a,*] *Brahim Mohammedi*,[b] *Salah Hanini*,[a] *Mouloud Boumahdi*,[a] *Ahmed Rezrazi*[a] i *Maamar Laidi*[a*]

Cilj ovog istraživanja bio je predvidjeti *otpor prljanja* primjenom *umjetnih neuronskih mreža* (ANN). Baza podataka za ANN modeliranje preuzeta je iz dostupne literature i sadrži podatke vezane uz prljanje kondenzacijskih cijevi u sustavu hlađenja morskom vodom u nuklearnoj elektrani. Sedam parametara korišteno je kao ulaz u neuronske mreže: bezdimenzijska temperatura morske vode, bezdimenzijski unutarnji ukupni koeficijent prijenosa topline, bezdimenzijski vanjski ukupni koeficijent prijenosa topline, bezdimenzijska temperatura kondenzatora, bezdimenzijski tlak u kondenzatoru, bezdimenzijska izlazna snaga i bezdimenzijska ukupna toplinska efikasnost. Kao izlaz uzet je bezdimenzijski otpor prljanja. Točnost modela potvrđena je statističkom analizom podudarnosti predviđenih i eksperimentalno dobivenih podataka. Rezultati su pokazali izvrsno slaganje u slučaju neuronske mreže sa 7 ulaza, 7 neurona u skrivenom sloju i 1 izlazom, uz korijen srednje kvadratne pogreške (RMSE) od $3{,}6588 \cdot 10^{-7}$, srednju apsolutnu postotnu pogrešku (MAPE) od 0,1295 % te visoki koeficijent determinacije ($R^2 = 0{,}99996$). Nakon provedene analize osjetljivosti (sve ulazne varijable imale su snažan utjecaj na procjenu otpora prljanja), s ciljem kontrole prljanja, uspostavljen je model *inverzne umjetne neuronske mreže* (ANNi); model je pokazao dobro slaganje za različite vrijednosti bezdimenzijske temperature morske vode.

Ključne riječi
Izmjenjivač topline-kondenzator, zagađivanje, modeliranje, umjetna neuronska mreža, grafičko korisničko sučelje, inverzna umjetna neuronska mreža

[a] *Laboratory of Biomaterials and Transport Phenomena (LBMPT) University of Médéa, 26 000 Alžir*
[b] *Nuclear Research Center of Birine Djelfa,17 000 Alžir*

Izvorni znanstveni rad
Prispjelo 1. prosinca 2020.
Prihvaćeno 25. veljače 2021.